Architectural Pattern, Characteristics and Binding Energies of Nuclides in Terms of Quarks of Quantum Chromo Dynamics

Bijon Kumar Sen* and Subha Sen*

Department of Chemistry, University of Calcutta, INDIA

Abstract:

The symmetry based architectural model of the nucleus explains the characteristics of the nuclides such as their nucleosyntheses, the radioactive emission phenomena, fission and fusion reactions without much involvement of intricate mathematics. Invoking the concept of d-quarks from Quantum Chromo Dynamics the structure, properties and binding energy of α-particle and those of low mass number nuclides could easily be derived. This is now being extended to heavy nuclides to reveal some of their characteristic phenomena regarding the dimension of nuclear shells, their non-uniform densities and the absence of mean free path among the nucleons. This model seems to be entirely different from the commonly adopted nuclear models. The description of the nuclear arrangement in architectural polyhedral model for all the elements starting from ^{4}He to ^{238}U shows perfect match between the capacity of the polyhedron and the number of d-quarks available. This concept is further applied to discuss the unique feature of most tightly bound "iron group of elements", comparison of the emission process of the radioactive disintegration products in different radioactive series and the properties of transactinide.

On the basis of the number of quarks involved, the binding energies of the possible isotopes of elements up to the transactinide are calculated. A few simple empirical formulae are proposed for the theoretical calculation of binding energies of the nuclides by evading several complex terms used in the classical Weizsäcker "mass formula". The closeness of the results with the experimental mass spectral binding energies has been established by comparison with nuclides taken at random from the entire range of known elements.

Key words: *Nuclear architecture, Nuclear Symmetry, Polyhedral model, Nuclear Binding by d-quarks, Fissionability of ^{235}U, Binding energy from empirical equations.*

---

*Retired, Address for correspondence DD - 114, Street no. 269, Action Area I, Newtown, Kolkata 700156, INDIA, E-mail: bk_sen@yahoo.com

Introduction:

The nucleus of an atom cannot be visualized by any experimental method or technique known to the nuclear scientists up till now. Many mathematical models were presented to describe the properties of the nucleus which are usually derived from the known properties or arrangement of extra-nuclear electrons. Of these models, most important are the gaseous shell model [1-3], the liquid drop model [4, 5], the collective model [6], the Fermi gas model [7] and the light scattering model [8, 9]. Although these models can individually explain some of the properties of the nuclei with reasonable degree of success, none of these is satisfactory for covering all aspects of nuclear properties and none of these can suggest visualization of the nuclei and the nucleosynthetic process. Attempts have been made to suggest through α- particle cluster model [10] and its variations [11-13] and a very recent lattice model [14] to provide some kind of structure of nuclei but these also failed to provide an all-inclusive solution to the problem.

An architectural pattern of the nucleus which is capable of visualization (albeit imaginary) based on the simple spatial symmetry has been proposed in an earlier communication [15]. This is considered to be formed from Bose-Einstein condensation of p – n pairs, which are different from ^{2}D (with spin 1) but its alternative form with spin 0 (termed Paulion) [16] following Pauli-Exclusion Principle. These p – n pairs along with n – n and n are arranged symmetrically to form successive polyhedral cages with increasing dimension. In order to supply the necessary binding energies to the nucleons in these polyhedrons, the idea of quarks of Quantum Chromo Dynamics have been invoked which successfully yielded the Binding Energies of α- particle and those of low mass number nuclides [17].

Binding force is the strong attractive force by which the nucleons are held together in a nucleus. Binding energy on the other hand is the energy required to disassemble a nuclide into its components (neutrons and protons). Thus, the binding force may be treated as the cause and

binding energy being its effect. Binding force is thought to be originated from exchange of some properties among the nucleons. The exchange may involve space (Majorana force), charge (isospin), spin (Bartlett), space and spin (Heisenberg) or ordinary non exchange (Wigner). This concept of exchange was proposed by Heisenberg in analogy with space and spin exchange in the formation of H_2 molecule, but was not justified on any fundamental basis when applied to nucleons. H. Yukawa [18] in 1935 proposed his meson theory of exchange in which π-meson (Pions) exchange produces the binding force between the nucleons. It was not explained whether the exchange is partial or complete.

The calculation of binding energy, is really a tricky problem. The usual method is to find the mass difference in the formation of the nuclide from its components and converting this "mass defect" into energy by using the famous Einstein equation $E = mc^2$. The energy calculated in this way includes the kinetic energy of the neutrinos and consequently imposes the difficulty in exact computation of the binding energy values. It is known that for $^2H_1$ (deuteron) the binding energy per nucleon is only 1.1123 MeV while for $^4He_2$ it is 7.074 MeV. Wigner justified that the low value of $^2H_1$ is due to the tendency of large positive kinetic energy to unbind the system. For $^4He_2$ nucleus the kinetic energy is not sufficient in comparison to the potential energy arising from 6 bonds between the nucleons. $^4He_2$ shows a binding energy of 28.7 MeV in the fusion reaction of $4H^+$ from which 0.511 MeV is taken away by the neutrino and the net binding energy corresponds to a value of ~ 28.2 MeV.

On the basis of the Liquid Drop Model, Weizsäcker [19] proposed his *empirical mass equation* for the determination of the mass of an atom as follows:

$$m(^AX_Z) = Z \text{ x mass of } H + (A - Z) \text{ x mass of neutron} - \Delta m$$

where Δm is the mass defect which can be expressed as $\Delta m = B/931$

In order to calculate the mass defect, it is necessary to know B, the binding energy of the system, which was expressed as the sum of energies arising from volume, surface, Coulomb, asymmetry and pairing terms described respectively in the following equation multiplied by empirical constants.

$$B = 14.1\ A - 13\ A^{2/3} - 0.595\ Z\ (Z - 1)\ A^{-1/3} - 19\ (A - 2\ Z)^2\ A^{-1} \pm \text{or } 0\ \ 135\ A^{-1}\ \text{MeV}$$

It is now necessary to distinguish between the binding energies calculated by the above expressions and the binding force among the nucleons by the exchange of π-meson between proton and neutron to produce the necessary binding force. Since a π-meson is about 270 times the mass of an electron, its complete transfer would produce enormous amount of binding energy which may lead to complete conglomeration of the nucleons. It seems that only a small fraction of the mass of the π-meson would be transferred (exchanged) to get the desired binding energy of the nucleons.

To understand the properties of the nucleus, a suitable architectural model is required for describing the arrangement of nucleons in a nucleus. Also, on the basis of the model, an acceptable value of the binding energy is to be ascertained. One such model is the polyhedral architectural model in which the nucleons can be arranged in a symmetrical disposition inside a few concentric cages.

Blueprint of the polyhedral architecture:

The architectural pattern of the nucleus is supposed to be formed by the entrapment of an α-particle within the polyhedral structures, viz., tetrahedron, cube, octahedron, dodecahedron and icosahedron successively. It is necessary to know the spacings of these polyhedrons, their capacity of holding nucleons, the radial distances and the arrangements of p – n and n – n pairs available. As any method of direct measurement of the spacings of the designs inside the nucleus is not possible, an approximate estimate of these is made by using

the root mean square radii values of different nuclides. The experimental values of these radii reported by Hofstadter [20] are shown in Table I and these are plotted against the corresponding mass number (Fig. I).

Table I: RMS radii of different nuclides

Nuclide	Nuclear Mass	RMS Radius (fm)	Nuclide	Nuclear Mass	RMS Radius (fm)
^{4}He	4	1.67	^{64}Zn	64	3.89
^{6}Li	6	2.51	^{88} Sr	88	4.22
^{12}C	12	2.47	^{89}Y	89	4.24
^{14}N	14	2.54	^{93}Nb	93	4.32
^{16}O	16	2.71	^{116}Sn	116	4.63
^{24}Mg	24	3.04	^{120}Sn	120	4.67
^{28}Si	28	3.13	^{139}La	139	4.86
^{40}Ca	40	3.49	^{142}Nd	142	4.90
^{48}Ti	48	3.60	^{184}W	184	5.32
^{52}Cr	52	3.65	^{197}Au	197	5.44
^{56}Fe	56	3.74	^{208}Pb	208	5.51
^{58}Ni	58	3.78	^{228} Ra	228	5.65

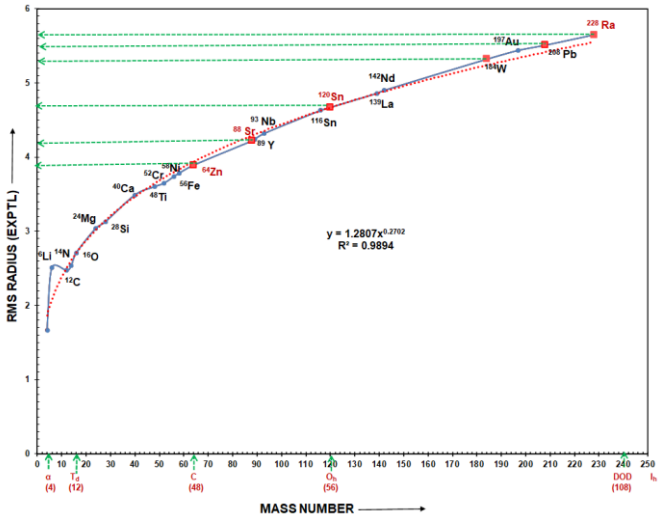

Fig. I: Plot of RMS Radii against Mass Number

From this plot, the radius value of some of the nuclides like Zn, Sr, Sn, W, Pb and Ra were extrapolated and included in Table I. The radius value at ^{4}He, ^{16}O, ^{64}Zn, ^{120}Sn and ^{228}Ra represents the radius value of α, T_d, Cube, O_h, DOD polyhedral cages respectively and are

included in Table II from which density values of different polyhedral shells have been computed.

TABLE II: Density values in different polyhedral shells in the nucleus

Type of polyhedron	Radius r (fm)	4/3 π [r_2^3 – r_1^3] = V	No. of nucleons	Density = No. of nucleons /V
α	1.67	19.499	4	0.205
T_d	2.71	63.826	12	0.188
Cube	3.89	163.118	48	0.294
O_h	4.63	169.095	56	0.331
DOD	5.65	339.578	120	0.353
I_h	--	--	--	

In Fig. II, the polyhedrons are schematically shown as spherical shells. These spherical shells cannot be compared with the extranuclear electronic "stationary states" because in the latter cases the electrons can move from one state to another by absorption or emission of energy. In the nuclear polyhedral states, this type of to and fro motion of α or β particles is not possible although γ-rays may be transmitted as these are associated with energy changes and are amenable to quantum mechanical rules. Fig. II (a) actually indicates the cross section of the spherical boundaries enclosing the polyhedral disposition. Fig. II (b) represents, an encompassed dodecahedral cage as an example.

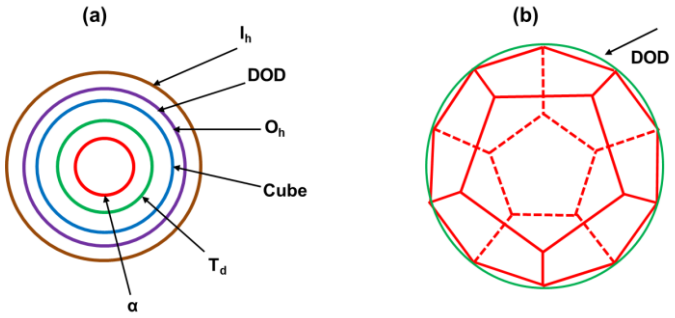

Fig. II: (a) Cross section of spherical shells. (b) DOD entrapped within a circle

While the electronic orbitals are guided by a central Coulomb field, which may be virtually present at the centre, the nucleus itself is not centrally guided by any such potential due to its non-uniform density. This non-symmetric distribution of nucleons as a whole in the nucleus gives rise to its electrical quadrupole moment,

Subshells at Ca, Sr, Ce, Tb, W and Pb are possible by the fulfillment of parts of different polyhedrons which are stable obeying symmetrical arrangements [15].

From the computed radii values, the volume of the annular spaces in the polyhedral cages can be determined by using the relation $V = 4/3\pi[(r_2)^3 - (r_1)^3]$. As these polyhedral spaces are occupied by different number of nuclides, the densities (nucl/fm^3) are calculated accordingly (Table II). The corresponding plot is shown in Fig. III.

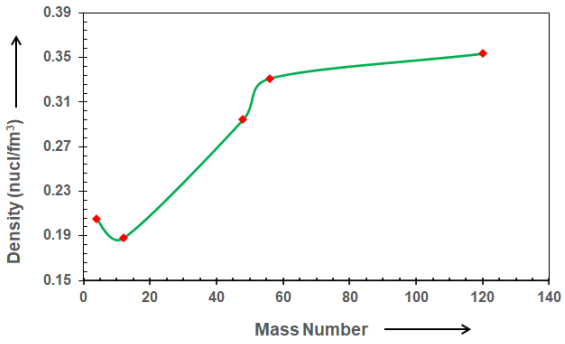

Fig. III: Plot of Density against Mass Number

In the gaseous and liquid drop models, the density values of the nuclei are considered to be uniform (0.17 nucl/fm^3). But the density values in Fig. III indicate the concentration of nucleons at a particular polyhedral cage and not the average value of the density of the nucleus. These non-uniform densities are expected as the polyhedral model assumes that nuclides are solids with rigid and compact structure built by the condensation of p – n pairs. These density values denote real material particles per volume in different strata of the nucleus and is completely different from the mathematical probability density mappings of the extranuclear electrons which describe the different shapes of s, p, d etc., orbital of electronic dispositions.

It is also notable that as the polyhedron model signifies compact structure of p – n pairs in the solid state, the question of mean free path of the particles does not arise. The vibrational modes of the protons and neutrons in the cages is quite possible as also the rotation of these particles along their own axes. But orbital revolutions of these particles as is considered in most of the accepted models do not appear to be reasonable in terms of the polyhedral model. Formation of 'holes' by the movement of nucleons is not ruled out and this suggests a mechanism for virtual to real α particle formation and also for β-emission by the interaction of a neutron with a p – n pair.

Nuclear architecture in terms of d-quarks:

In a previous communication [17], the formation and structure of α-particle was shown to be guided by the number of d-quarks available in the system. This concept was extended to explain the formation of isotopes of low mass number nuclides. It can now be shown that this process of linking between the number of quarks available and the arrangement of nucleons in a suitable polyhedral system also holds good for nuclides of all elements starting from ^{4}He up to ^{238}U. The total capacity of the polyhedron (Table III) to accommodate nucleons (proton and neutron) in the sequence of α, T_d, Cube, O_h and DOD cages are 4 (He) 12 (Li to O), 56 (O to Zn), 62 (Zn to Sn) and 128 (Sn to U). The respective capacity of the polyhedrons in terms of quarks (3 d-quarks per neutron present in the nuclide) comes out to be 6, 18, 96, 102 and 222 that arise from the accommodation of 3 quarks per side (p – n), 3 quarks per corner (n) and 6 quarks per face (2 (p – n pairs) of the particular type of polyhedron. These are indicated in Table III which shows a direct connection between the number of quarks in the nuclides and the capacity of nucleons in the resulting polyhedron structure. A complete match between the two is revealed. Thus, the total capacity of d-quarks up to dodecahedral structure is 6 + 18 + 96 + 102 +222 = 444. Out of these, 438 quarks are utilized in building the structure of ^{238}U and the remaining 6 quarks can account for the existence of stable isotope of ^{240}U.

Table III: Matching of Nuclides with Polyhedral Model via d -quarks

Nuclide $^{A}X_{Z}$	No. of Excess Neutron (A-2Z)	No. of d-quarks 3 (A-Z)	Type of Polyhedron	No. of Sides, S Corners, C & Faces, F with capacity of Nucleons	Maximum Capacity of d-quarks in Polyhedra	Distribution of quarks in Polyhedra	Total d-quarks in the Nuclide
$^{4}He_{2}$	0	6		4	6	α (6)	6
$^{16}O_{8}$	0	24	T_d	6 S (12)	18	α (6) S (18) = [T_d]	24
$^{40}Ca_{20}$	0	60	Cube	12 S (24) 8 C (8) 6 F (24)	36 + 24 +36 = 96	[T_d] S (36)	60
$^{64}Zn_{30}$	4	102	″	″		[T_d] S (36) C (6) F (36) = [Cube]*	102
$^{88}Sr_{38}$	12	150	O_h	12 S (24) 6 C (6) 8 F (32)	36 +18 + 48 = 102	[Cube]* S (36) C (12)	150
$^{120}Sn_{50}$	20	210	″	″		[Cube] S (36) C (6) F (48) = [O_h]*	210
$^{140}Ce_{58}$	24	246	DOD	30 S (60) 20 C (20) 12 F (48)	90 +60 +72 = 222	[O_h]** S (30)	246
$^{159}Tb_{65}$	29	282	″	″		[O_h] S (60)	282
$^{182}W_{74}$	34	324	″	″		[O_h] S (90) F (12)	324
$^{208}Pb_{82}$	44	378	″	″		[O_h]** S (90) F (72)	378
$^{220}Rn_{86}$	48	402	″	″		[O_h]* S (90) C (30) F (72)	402
$^{238}U_{92}$	54	438	″	″		[O_h] [DOD]*	438
$^{240}U_{92}$	56	444	″	″		[O_h] [DOD]	444

The detailed breakup of the distribution of quarks in the polyhedrons are shown as follows:

[T_d] = α (6) T_d (18) = 24;

[Cube]* = [T_d] S (36) C (6) F (36) = 102;

[Cube] = [Cube]* C (18) = [T_d] S (36) C (6) F (36) C (18) = 120;

[O_h]* = [Cube] S (36) C (6) F (48) = [T_d] S (36) C (6) F (36) C (18) S (36) C (6) F (48) =210;

[O_h]** = [O_h]* C (6) = [T_d] S (36) C (6) F (36) C (18) S (36) C (6) F (48) C (6) =216;

[O_h] = [O_h]** C (6) = [T_d] S (36) C (6) F (36) C (18) S (36) C (6) F (48) C (6) C (6) = 222;

[DOD]* = 216
[DOD] = 222

} The occupancy of these quarks among the sides and faces of the DOD will depend on the nuclides with the corners mostly vacant (vide Table VI).

Table III shows that α-particle with 6 quarks is entrapped tetrahedrally by 12 quarks to produce oxygen which is surrounded by a cube with 96 quarks to produce ^{64}Zn which in turn is surrounded by 108 quarks to produce ^{120}Sn in a complete octahedral structure. Ultimately this is then encompassed by a dodecahedral disposition of 222 quarks to produce ^{240}U.

To account for the structural disposition of transuranic elements, a peripheral icosahedral arrangement is needed to be considered but these are not shown in the Table as not enough number of nuclides are known to fill the icosahedron completely.

It has been stated earlier [15] that while the sides and faces of the bigger polyhedrons are occupied by p – n pairs, the corners accommodate the excess neutrons required for the stability of the nuclides. The p – n pairs in the faces are positioned in a crosswise arrangement to form virtual α-particles which could easily be converted to real α- particles under appropriate conditions and could be emitted as α-particles. It is the arrangement of neutrons in a symmetric fashion in the polyhedron which produces relatively stable nuclides. As is evident from the Table, the capacity of quarks in different polyhedrons may be written as follows: [Td] = 24, [Cube]* = 102, [Cube] = 120, [O_h]* = 210, [O_h]** =216, [O_h] = 222, [DOD]* = 216 and [DOD] = 222. The difference in the arrangements of nucleons in a particular polyhedron depends on how the neutrons are arranged in a strictly symmetrical fashion e.g., in a cube, the eight corners may be occupied either by four in a tetrahedral disposition or by eight in a completely filled cubic arrangement. In O_h, the corners are occupied either by 2, 4 or 6 neutrons to form a symmetrical arrangement. In a dodecahedron, the corners may accommodate either 10 or 20 neutrons. The sides of course are occupied by p – n – pairs or n – n pairs in a symmetrical way. In Table III, some of the important nuclides are shown along with their symmetric quark distribution. The nuclide $^{220}Rn_{86}$ (isotopic with $^{222}Rn_{86}$) which is usually known as Thoron derived from radioactive disintegration of $^{232}Th_{90}$ is also included.

Iron Group of Elements:

The nuclides of some elements around mass number 60 with even A and even Z comprising of Ni, Cr and Fe are found to be most tightly bound nuclei among all elements with high values of B/A (Binding energy/Nucleon). These nuclides known as "Iron group of elements" are listed in Table IV along with symmetrical distribution of the outermost d-quarks and their reported binding energy per nucleon (B/A) values [21]. The reported experimental binding energy of each nuclide is compared with the binding energy values calculated by using the proposed empirical formula (*vide infra*).

Table IV: Distribution of d-quarks in Fe group of nuclides

Nuclide	B/A (MeV)	Abun-dance (%)	B. E. Expt.	B. E. Calc.	No. of d-Quarks	Distribution of d-quarks	Peripheral Nucleons
$^{62}Ni_{28}$	8.795	3.6	545.3	541.4	102	$[T_d]$ S (36) C (**18**) F (24)	2 α, 4 p – n
$^{60}Ni_{28}$	8.780	26.2	526.8	511.2	96	$[T_d]$ S (36) C (12) F (24)	2 α, 4 p – n
$^{58}Ni_{28}$	8.732	68.1	506.5	481.0	90	$[T_d]$ S (36) C (**6**) F (24)	2 α, 4 p – n
$^{60}Fe_{26}$	8.755	trace	525.3	539.4	102	$[T_d]$ S (36) C (24) F (18)	6 p – n
$^{58}Fe_{26}$	8.792	0.3	509.9	509.2	96	$[T_d]$ S (36) C (**18**) F (18)	6 p – n
$^{56}Fe_{26}$	8.790	91.8	492.2	479.0	90	$[T_d]$ S (36) C (12) F (18)	6 p – n
$^{54}Fe_{26}$	8.736	5.9	471.7	448.8	84	$[T_d]$ S (36) C (**6**) F (18)	6 p – n
$^{54}Cr_{24}$	8.715	2.4	470.6	477.0	90	$[T_d]$ S (36) C (**18**) F (12)	4 p – n
$^{52}Cr_{24}$	8.776	83.8	456.4	446.8	84	$[T_d]$ S (36) C (12) F (12)	4 p – n

$[T_d] = \alpha\ (6)\ T_d\ (18) = 24$ Unsymmetrical fillings of corners are marked with bold face.

^{62}Ni is the most tightly bound nuclide in terms of B/A values followed by ^{58}Fe and ^{56}Fe. It was a misnomer that ^{56}Fe is the "most stable nucleus" among all nuclides. In fact, this isotope has the lowest *mass per nucleon* of all nuclides (not binding energy per nucleon), which is 930.412 MeV/c^2, accompanied by ^{62}Ni with 930.417 MeV/c^2 and ^{60}Ni with 930.420 MeV/c^2 respectively. While in ^{56}Fe, the percentage of proton is higher than that in ^{62}Ni, the latter has a greater proportion of neutrons which are more massive than protons. This lowers the mean mass-per-nucleon ratio in ^{56}Fe in a way that has no effect on its binding energy.

Among the stable Fe isotopes, $^{56}Fe_{26}$ is the most abundant (91.75%) followed by lesser abundant ^{54}Fe (5.85%), ^{54}Fe (2.12%) and ^{58}Fe (0.28%). ^{56}Fe is unique in that it has the highest available binding energy among stable nuclides which is justified by its compact symmetrical disposition of nucleons in the polyhedral model. The radioactive nuclide ^{60}Fe with a half-life of 2.26 million years is believed to be synthesized in massive stars, with the gamma rays associated with its decay have been detected by gamma-ray space observatories.

Both ^{62}Ni and ^{60}Fe have the same number of quarks (102) and the distribution of d-quarks among the polyhedral shells are shown in Table IV. Both of these are "extinct radionuclide" which are formed by primordial process in the early solar system approximately 4.5 billion years ago and became extinct by photodisintegration in the lifetime of the universe in the span of several half-life periods [22,23].

$^{56}Fe_{26}$ and $^{54}Cr_{24}$ both have 90 quarks each, but the stability of the latter is less due to the presence of unsymmetric disposition of neutrons in the latter.

The structures of $^{56}Fe_{26}$, along with those of $^{182}W_{74}$, $^{238}U_{92}$ and $^{199}Au_{79}$ are shown in Fig. IV.

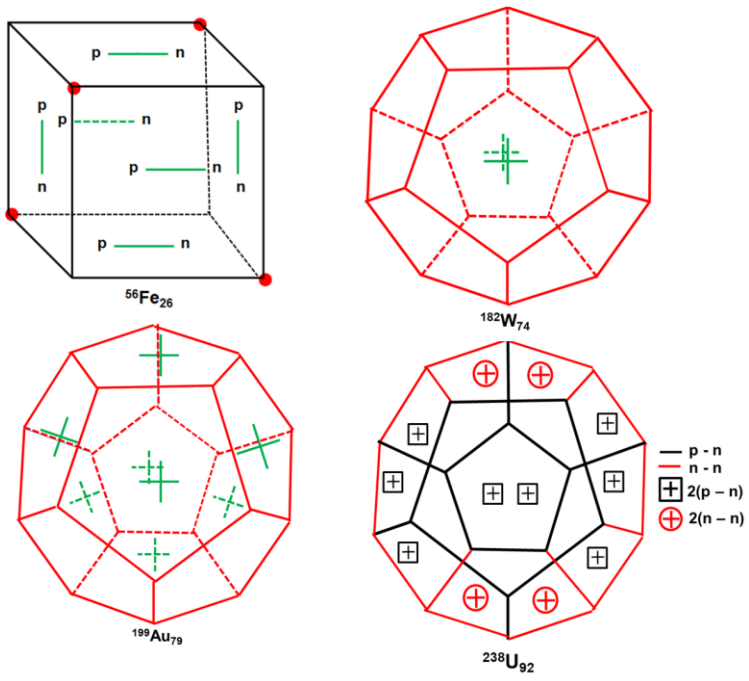

Fig. IV Disposition of outermost nucleons in $^{56}Fe_{26}$, $^{182}W_{74}$, $^{199}Au_{79}$ and $^{238}U_{92}$

(a) $^{56}Fe_{26}$ shows the presence of 4 extra neutrons in tetrahedral position.

(b) In $^{182}W_{74}$, all the sides (30) of the dodecahedral structure along with 14 corners lying in the interior cube (8) and octahedron (6) are filled up by 90 and 42 quarks respectively. Only two faces of the dodecahedron are occupied by 12 quarks. All the corners of dodecahedron structure remain vacant. In an earlier communication [15] this was thought to be ^{181}Ta but considering the concept of quarks, ^{182}W would be a better fit.

(c) In $^{199}Au_{79}$, 8 of the12 dodecahedron faces are occupied by virtual α-particle to form symmetrical structure.

(d) In $^{238}U_{92}$, all the 12 dodecahedron faces are occupied by virtual α-particle.

It is to be noted that the disposition of p – n pairs and n – n pairs in the polyhedrons are not unique. It is quite possible to present other arrangements keeping the number of quarks unchanged and maintaining the symmetrical occupancy of polyhedrons by nucleons as far as practicable.

Radioactive disintegration products in terms of quarks and architectural model:

The nuclide $^{228}Ra_{88}$ loses 5 α and 4 β^- to produce $^{208}Pb_{82}$ as is seen in Th (4n + 0) series (Cf. Table VA).

$$^{228}Ra_{88} \xrightarrow[-\ 4\ \beta]{-\ 5\ \alpha} {}^{208}Pb_{82}$$

Similarly, in (4n + 2) series, ^{238}U by losing 8 α and 6 β^- gives rise to $^{206}Pb_{82}$.

The decay of naturally occurring 4n + 2 (Uranium) and 4n + 0 (Thorium) series can be depicted in a condensed way as shown in the following disintegration pattern:

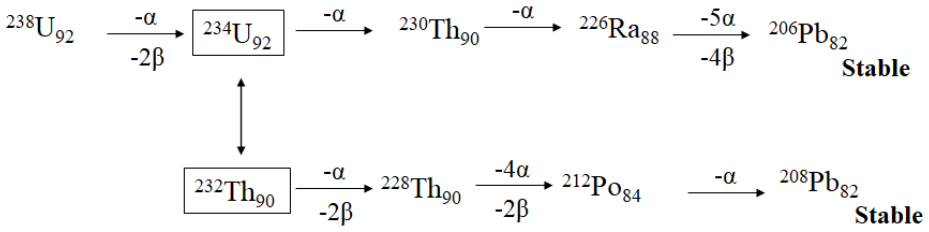

Both $^{234}U_{92}$ and $^{232}Th_{90}$ are bonded by 142 x 3 = 426 quarks There are only two possible ways of arranging the distribution of these quarks among the polyhedral structures in a symmetric fashion as follows.

Serial no.	α	T_d	Cube			Octahedron			Dodecahedron			Total
			S	C	F	S	C	F	S	C	F	
1.	6	+ 18	+ 36	+ 12	+ 36	+ 36	+ 12	+ 48	+ 90	+ 60	+ 72	426
2.	6	+ 18	+ 36	+ 24	+ 36	+ 36	+ 0	+ 48	+ 90	+ 60	+ 72	426

This shows that the process of radioactive disintegration of the nuclides is case specific and is very much dependent on the distribution of quarks in the polyhedral structure. These two isotopes have almost identical values of binding energies of ~1770 MeV (vide Table VA) but their disintegration properties are widely different. Thus, half-life value of the U isotope is ~ 0.244 My while that of Th isotope is 14.05 Gy. This high value of Th isotope suggests that the arrangement of nucleons in this corresponds to arrangement 2 above where a compact structure is observed with the inner cubic corners are fully occupied by 24 neutrons.

Comparison of disintegration series in terms of quarks:

There are four known disintegration series of radioactive elements viz., Np, Ac, U and Th series of which the neptunium series is considered to be artificial due to the fact the starting isotope $^{237}Np_{93}$ is produced artificially. In spite of its high value of half-life (2.14 My), it has become extinct in terrestrial condition due to its natural decay in the lifetime of the universe. This series along with others designated as 4n + 1, 4n + 2, 4n + 3 and 4n + 0 series are arranged in Table VA in vertical columns along with the number of d-quarks in rows. The calculated

and experimental binding energies of the nuclides are also included. The half-life periods of all these nuclides are indicated by the side of the symbols.

The members of these series are arranged in rows so that the number of d-quarks in each row is the same. The nuclides in a particular row in the Table may be considered as isotones as they contain the same number of neutrons and as isoergic nuclides having almost same binding energy arising from the exchange interaction. Slight difference in these values arises from the Columbic interaction of u- and d- quarks. From the number of quarks, their binding energies are calculated by using the proposed empirical formula (*vide infra*) and are compared with the experimental values as reported in [24]. The calculated values are quite close to the experimental ones.

It is seen that in each series of disintegration, the isotopes are mostly long lived up to the attainment of Ra nuclide after which the daughter elements are very short lived and quickly attain a nuclide of either Bi or Pb which are stable and non-radioactive. From ^{238} U to ^{228}Ra, the isotopes are stable as this conforms to relatively stable nucleonic arrangement in the dodecahedral structure but after Ra the disintegration becomes quicker. Up to Ra, the nuclides may be considered to be in secular equilibrium while those from Ra to Pb or Bi are present in transient equilibrium.

In all the four radioactive disintegration series, some nuclides show both α and β emission properties. These are characteristics of the nuclides which are short lived and are in transient equilibrium. The classification of these nuclides according to their number of d-quarks content is shown in Table VB. Some of the short-lived nuclides for which the experimental binding energy is not reported in the literature are included along with expected values calculated for the proposed empirical equation.

Table VA: Properties of disintegration products and their binding energies in terms of quarks

No of Quarks	Artificial 4n + 1 Neptunium Series	Natural 4n +2 Uranium Series	Natural 4n +3 Actinium Series	Natural 4n + 0 Thorium Series	Average B. E. Calc.*	Average B. E. Expt.
438		$^{238}U_{92}$ 14.47 Gy			1821	1802
		↓ -α				
432	$^{237}Np_{93}$ 2.14 My	$^{234}Th_{90}$ 24.1 d			1795 #	1795 #
429	↓ - α	↓ - α	$^{235}U_{92}$ 1704 My		1781	1784
426	$^{233}Pa_{91}$ 27d	$^{234}U_{92}$ 0.244 My	↓ - α	$^{232}Th_{90}$ 14.05 Gy	1769 #	1773 #
	↓ - β					
423	$^{233}U_{92}$ 0.159 My	↓ - α	$^{231}Th_{90}$ 25.6 d	↓ - α	1756 #	1766 #
	↓ - α		↓ - β			
420		$^{230}Th_{90}$ 7700 y	$^{231}Pa_{91}$ 32500 y	$^{228}Ra_{88}$ 5.75 y	1744 #	1758 #
417	$^{229}Th_{90}$ 7340 y	↓ - α	↓ - α	↓ - 2 β	1731	1748
414	↓ - α	$^{226}Ra_{88}$ 1600 y	$^{227}Ac_{89}$ 21.8 y	$^{228}Th_{90}$ 1.913 y	1719 #	1735 #
411	$^{225}Ra_{88}$ 18.4 d		↓ - α	↓ - α	1707	1725
408			↓ - β	$^{224}Ra_{88}$ 3.64 d	1694	1720
405			$^{223}Ra_{88}$ 11.43 d		1681	1714
	↓ - 4 α - 3 β	↓ - 5 α - 4 β	↓ - 4 α - 2 β	↓ - 4 α - 2 β		
	$^{209}Bi_{83}$	$^{206}Pb_{82}$	$^{207}Pb_{82}$	$^{208}Pb_{82}$		

* Calculated Binding Energy = (A - Z) x 14.1 – A; # Mean value of Binding Energy for nucleons with same number of d-quarks

Table V B: Properties of disintegration products in transient equilibrium

No. of quarks	4n +1	4n +2	4n +3	4n +0	B.E. Cal.	B.E. Exp.
414			$^{227}Ac_{89}$		1719	1737
411			$^{227}Th_{90}$		1705	N. A
408			$^{223}Fr_{87}$		1695	1714
405			$^{223}Ra_{88}$		1681	1714
402		$^{218}Po_{84}$	$^{219}At_{85}$		1671*	N. A
399		$^{218}At_{85}$	$^{219}Rn_{86}$		1657*	N. A
396		$^{214}Pb_{82}$	$^{215}Bi_{83}$		1647*	N. A
393		$^{214}Bi_{83}$	$^{215}Po_{84}$		1633*	N. A
390	$^{213}Bi_{83}$	$^{214}Po_{84}$	$^{215}At_{85}$		1619*	N. A
387	$^{213}Po_{84}$	$^{210}Tl_{81}$	$^{211}Pb_{82}$	$^{212}Bi_{83}$	1607*	N. A
384	$^{209}Tl_{81}$	$^{210}Pb_{82}$	$^{211}Bi_{83}$	$^{212}Po_{84}$	1594*	1648*
381	$^{209}Pb_{82}$	$^{210}Bi_{83}$	$^{211}Po_{84}$	$^{208}Tl_{81}$	1580*	1643*
378	$^{209}Bi_{83}$	$^{210}Po_{84}$	$^{207}Tl_{81}$	$^{208}Pb_{82}$	1568*	1637*
375		$^{206}Tl_{81}$	$^{207}Pb_{82}$		1556*	1625*
372		$^{206}Pb_{82}$			1541	1629

——— Indicates α- emission and --------Indicates β- emission; *Mean value of B.E. for nucleons with same number of d-quarks

Fissionability of ^{235}U and ^{239}Pu:

The proposed polyhedral architectural model of the nucleus consisting of α, T_d, Cube, O_h and DOD cages in succession has the capability of holding 148 neutrons and 114 protons altogether. $^{289}Fl_{114}$ is the most stable known isotope of the superheavy synthetic element Flerovium, which has 175 neutrons (525 quarks). Availability of 148 neutrons (444 quarks) in dodecahedral periphery is just sufficient to accommodate $^{240}U_{92}$. A few more isotopes of nuclides of transuranic elements can be accommodated in the dodecahedral cage provided that their neutron numbers do not cross 148. The distribution of nucleons in some radioactive nuclides is shown in Table VI that shows the presence of dineutrons (n – n) for the stability overcoming the repulsion of protons and thereby produce a symmetrically stable periphery leaving many corners vacant within the polyhedral cages.

Table VI: Distribution of nucleons in some radioactive nuclides

Nuclide	No. p – n	α	T_d	Cube			Octahedron			Dodecahedron		
	No. n			S	C	F	S	C	F	S	C	F
$^{228}Ra_{88}$	88 p – n	2	6	12	-	12	12	-	16	16	-	12
	52 n	-	-	-	-	-	-	-	-	14 nn	-	12 nn
$^{235}U_{92}$	92 p – n	2	6	12	-	12	12	-	16	16	-	16
	51 n	-	-	-	8n	-	-	-	-	14 nn	-	7 nn + n
$^{237}Np_{93}$	93 p – n	2	6	12	-	12	12	-	16	17 + n	-	16
	51 n	-	-	-	8n	-	-	-	-	13nn	-	8nn
$^{238}U_{92}$	92 p - n	2	6	12	-	12	12	-	16	16	-	16
	54 n	-	-	-	8n	-	-	2n	-	14 nn	-	8 nn
$^{239}Pu_{94}$	94 p – n	2	6	12	-	12	12	-	16	17 + n	-	17
	51 n	-	-	-	8n	-	-	2n	-	13nn	-	7nn
$^{240}U_{92}$	92 p - n	2	6	12	-	12	12	-	16	16	-	16
	56 n	-	-	-	8n	-	-	4n	-	14 nn	-	8 nn
$^{243}Am_{95}$	95 p – n	2	6	12	-	12	12	-	16	17 + n	-	18
	53 n	-	-	-	8n	-	-	6n	-	13nn	-	6nn

S = Sides ; C = Corners ; F = Faces of Polyhedron

The arrangement for ^{235}U is interesting in that it shows an excess of one neutron in the peripheral dodecahedron structure. This odd neutron may well combine with a p – n to form ^{3}H leaving one place vacant in the peripheral pentagon. This ‘defect’ allows an external neutron

of low energy to enter the nucleus to produce fission reactions. In ^{238}U and ^{240}U, no such defects are present and any neutron from outside is scattered from the surface and no fissionability is observed ordinarily.

Similar is the case with $^{237}Np_{93}$, $^{239}Pu_{94}$ and $^{243}Am_{95}$ that shows the presence of one extra neutron each in the peripheral structure. Combination of this odd neutron with a p – n forms β^- active ^{3}H. In fact, these three nuclides are β^- active in addition to their usual radioactive property as α emitters.

As stated, ^{237}Np, ^{239}Pu and ^{243}Am with 144, 145, 148 neutrons and 432, 435 and 444, respectively (Cf. Table VII) can also be accommodated in the dodecahedral cage. This might probably be the reason for which Fermi's experiments to prepare transuranic elements by bombarding Uranium nuclei with slow neutrons could produce only Neptunium and Plutonium nuclides.

Transactinide Nuclides:

The polyhedral architectural model of the nucleus is further extended to transactinide nuclides staring from Ac_{89} up to Og_{118}. Beyond $^{243}Am_{95}$, all other known transactinide nuclides require more than 444 quarks for stability and therefore, they are required to be fitted in the next icosahedral cage. The icosahedron has the capacity of holding 246 quarks and thus is capable of accommodating many more transactinide nuclides than is known (Z = 118) at the present time. 30 sides of the icosahedral cage (built up by 30 p – n pairs of nuclides) is enough to house transactinide elements from $^{247}Cm_{96}$ to $^{294}Og_{118}$ leaving many places vacant in the corners and faces of the icosahedron. A loosely bound structure is thus produced with instability in the form of α and β emissions.

From Ac_{89} to Lr_{103} (formerly Lw), the elements are usually considered as the member of the 6f series parallel to the rare earth 5f series from La to Lu. The rest of the transactinide

elements from $^{261}Rf_{104}$ - $^{294}Og_{118}$ are obtained synthetically in small numbers mostly by American and Russian scientists. Elements up to Z = 126 has been predicted but their detailed characteristics are not yet definitely known.

The characteristics of the transactinide elements as regards to their number of quarks and their calculated binding energies are shown in Table VII.

Table VII: Trans-actinide elements and their Binding Energies

Name of the nuclide	**Symbol**	**Ex-cess Neut ron**	**No. of d-quarks**	**B.E. (MeV) Calc.**	**Name of the nuclide**	**Symbol**	**Ex-cess Neut ron**	**No. of d-quarks**	**B.E. (MeV) Calc.**
Actinium	$^{227}Ac_{89}$	138	414	1718.8	Rutherfordium	$^{261}Rf_{104}$	157	471	1952.7
Thorium	$^{232}Th_{90}$	142	426	1770.2	Dubnium	$^{262}Db_{105}$	157	471	1951.7
Protactinium	$^{231}Pa_{91}$	140	420	1743.0	Seaborgium	$^{266}Sg_{106}$	160	480	1990.0
Uranium	$^{238}U_{92}$	146	438	1820.6	Bohrium	$^{264}Bh_{107}$	157	471	1949.7
Neptunium	$^{237}Np_{93}$	144	432*	1793.4	Hassium	$^{277}Hs_{108}$	169	507	2105.9
Plutonium	$^{244}Pu_{94}$	150	450	1871.0	Meitnerium	$^{268}Mt_{109}$	159	477	1973.9
Americium	$^{243}Am_{95}$	148	444*	1843.8	Darmstadtium	$^{281}Ds_{110}$	171	513	2130.1
Curium	$^{247}Cm_{96}$	151	453	1882.1	Roentgenium	$^{272}Rg_{111}$	161	483	1998.1
Berkelium	$^{247}Bk_{97}$	150	450	1868.0	Copernicium	$^{285}Cn_{112}$	173	519	2154.3
Californium	$^{251}Cf_{98}$	153	459	1906.3	Nihonium	$^{286}Nh_{113}$	173	519	2153.3
Einsteinium	$^{252}Es_{99}$	153	459	1905.3	Flerovium	$^{289}Fl_{114}$	175	525	2178.5
Fermium	$^{257}Fm_{100}$	157	471	1956.7	Moscovium	$^{290}Mc_{115}$	175	525	2177.5
Mendelevium	$^{258}Md_{101}$	157	471	1955.7	Livermorium	$^{293}Lv_{116}$	177	531	2202.7
Nobelium	$^{259}No_{102}$	157	471	1954.7	Tennessine	$^{294}Ts_{117}$	177	531	2201.7
Lawrencium	$^{262}Lr_{103}$	159	477	1979.9	Oganesson	$^{294}Og_{118}$	176	528	2187.6

The binding energy of these transactinide nuclides are calculated from proposed empirical formula (A - Z) x 14.1 - A where A is the mass number and Z is the number of protons, 14.1 is the co-efficient which represents the value of the binding energy of three quarks (each with 4.7 MeV) as described later in this paper.

The plot of the binding energies of these transactinide elements against their mass number is shown in the Figure V which shows linear correlation with slight deviation from the straight line indicating uniform change and justified the use of the proposed empirical equation.

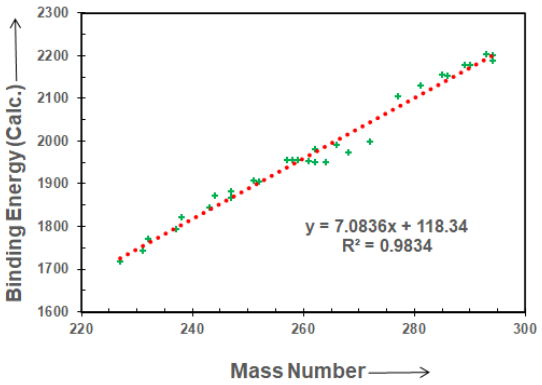

Fig. V: Plot of Calculated Binding Energies of Transactinide against Mass Number

The "Gold Rush" by Alchemists:

Lured by the beautiful lustre and rust resistant properties of gold, pseudoscientists (Alchemists) of India and China tried to prepare the metal from other entities before the start of Christianity. This practice was spread through Egypt, Greece, Syria and then to the Western Europe and lasted till 1700 A.D. All these efforts failed because of the fact that chemical reactions can bring about only cosmetic changes by affecting the extra-nuclear electronic structures with practically no effect on the nucleus of the atoms. Gold with isotopic configuration $^{199}Au_{79}$ is well protected in the periodic table by Pt metals (Os, Ir, and Pt) from the lower side and by the heavy metals (Hg, Tl, Pb, Bi) from the upper side. The gold nuclide ^{199}Au could perhaps be prepared from ^{207}Pb which is the end product of 4n +3 Actinium series by making it to lose 2α and 1 β^- but for the fact that ^{207}Pb is stable and till now no technique is known to the scientists for producing *controlled nuclear engineering*. Even if this is somehow attained, the economic viability would be the final question besides the disastrous impact of this 'artificial gold' on world economy.

The idea of 'touch stone' or 'philosopher's stone is nothing but a myth as it is not possible for a stony substance to change ^{56}Fe to ^{199}Au by a mild touch. The description of the gold nuclide can be represented as $^{199}Au_{79}$ = [Oh] S (90) F (48) with 8 virtual α-particles occupying 8 positions in the 12 dodecahedral faces in the outermost periphery. The peripheral structure of $^{199}Au_{79}$ is shown in Fig. IV.

Calculation of Binding Energies in terms of d-quarks:

In a previous communication [17], the process of formation of α-particle was discussed in terms of d-quarks. It was shown that the exchange of these quark particles can impart the required binding energy to the α-particles.

It was also shown earlier [15-16] that nuclides are built up by combining hypothetical particles termed *Paulion* (p – n pair) formed by the application of Bose-Einstein condensation process. Symmetrical arrangement of these particles inside a few polyhedral cages can give rise to a rigid nuclear architectural framework. The proposed architectural model is capable of explaining many of the nuclear phenomenon like emission, fission and fusion and process of nucleosyntheses. Invoking the concept of quarks from Quantum Chromo Dynamics it was possible to explain most of the characteristic uniqueness of α-particle. The exact binding energy of α-particle could also be predicted. This concept was extended qualitatively for the elucidation of the formation and properties of nuclides with low mass number (up to oxygen). Taking a cue from α-particle it has now been possible to calculate the binding energies of the nuclides of almost all mass number (including transactinide elements).

At the beginning of this communication, the "*semi-empirical mass formula*" of Bethe and Weizsäcker [19] for the calculation of nuclear mass and its binding energy is discussed. The related formula containing several terms representing 1) volume binding energy 2) surface

energy, 3) Coulomb energy 4) asymmetric energy and 5) pairing energy are expressed as follows:

$$B = 14.1\ A - 13\ A^{2/3} - 0.595\ Z\ (Z - 1)\ A^{-1/3} - 19\ (A - 2\ Z)^2\ A^{-1} \pm \text{or } 0\ \ 135\ A^{-1}\ \text{MeV}$$

The first term represents the volume energy which is obtained by multiplying mass number of the nuclide with an empirical constant 14.1. This, however, leads to a high binding energy as well as a high mass value. In order to reduce the high value of energy/mass it was necessary to consider other factors in the above formula. A close look at the volume energy term reveals an interesting coincidence that this constant equals the energy value of 3 quarks (3 x 4.7 MeV = 14.1 MeV). This idea is utilized to calculate the binding energies of the nuclides in a qualitative manner with the help of a few simple empirical equations.

The calculation is done by considering the number of quarks involved in the formation of the nuclides by using the relation B.E. (Theo) = (A - Z) 14.1 where (A – Z) represents the number of electrons equivalent to excess neutrons present in the nuclide which when multiplied by the binding energy value of three quarks (4.7 x 3 = 14.1) gives rise to the desired value of the binding energy of the nuclide. The theoretical values are calculated by using this formula and compared with the experimental values as reported by Martin [24] by plotting the mass number of the nucleons in Fig. VI.

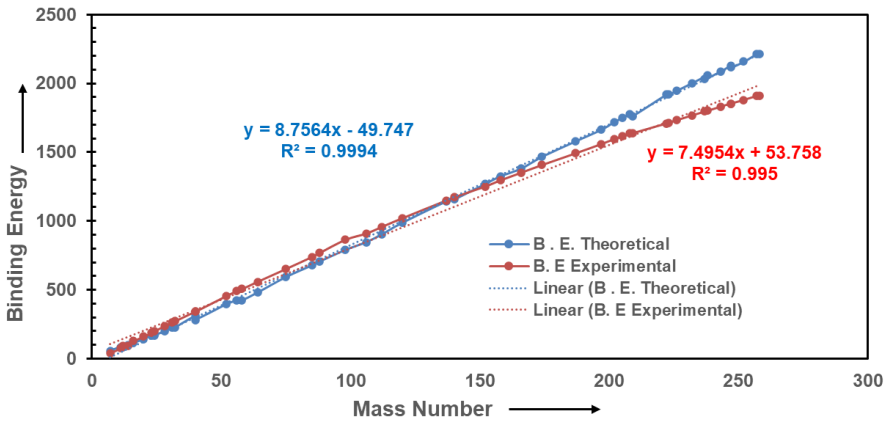

Fig. VI: Plot of Binding Energies for all Mass Numbers

The plot exhibits the following trends in the values:

a) Up to ~ $A \leq 60$ the calculated values are less than the experimental values.

b) In the region $60 < A < 200$, the values are more or less same in both the cases.

c) When $A \geq 200$, the calculated values are greater than the experimental value.

This definitely indicates that the binding energy is not contributed by the exchange of quarks alone but some other factor is also involved. This additional factor is the Coulombic interaction between the u - and d- quarks of the nucleons participating in the formation of p – n or n – n pairs.

In the case of (a), the nuclides contain an equal number of neutrons and protons so that there is a strong interaction between u- and d- quarks and this exchange contributed to the calculated binding energy. In case of (b) when $60 < A < 200$ the nuclides have excess neutrons for the stability. In this region the exchange force persists and the Coulombic interaction is mostly balanced by the repulsive effect of u-quarks present in the extra neutrons. In case of (c) with $A \geq 200$, the calculated binding energy values derived from quarks are greater than the experimental binding energy values. This is due in part from the repulsive Coulombic interaction between the protons which are present in high numbers and also due to the contribution from the repulsive effect of u-quarks present in the excess neutrons.

On the basis of these observations three simple empirical relations are proposed to calculate the B.E. in terms of d-quarks present in the nuclides. These relations are:

$$\text{B.E. (Theo.)} \longrightarrow \begin{cases} (A - Z)\,14.1 + A & \sim A \leq 60 \\ (A - Z)\,14.1 & 60 < A < 200 \\ (A - Z)\,14.1 - A & A \geq 200 \end{cases}$$

Tables VIII-X and the Figures VII-X show the matching of the calculated and the experimental values which appears to be quite satisfactory.

Table VIII: Matching of binding energies for nuclides with mass number A ≤ 60

Isotope	Z	A	B. E. Theo.	B. E. Exp.	Isotope	Z	A	B. E. Theo.	B. E. Exp.
^{7}Li	3	7	63.4	39.3	^{28}Si	14	28	225.4	236.5
^{11}B	5	11	95.6	76.2	^{31}P	15	31	256.6	262.9
^{12}C	6	12	96.6	92.2	^{32}S	16	32	257.6	271.8
^{14}N	7	14	112.7	92.2	^{40}Ar	18	40	350.2	343.8
^{16}O	8	16	128.8	127.6	^{40}Ca	20	40	322.0	342.1
^{20}Ne	10	20	161.0	160.6	^{52}Cr	24	52	446.8	456.3
^{23}Na	11	23	192.2	186.6	^{56}Fe	26	56	479.0	492.3
^{24}Mg	12	24	193.2	198.3	^{58}Ni	28	58	481.0	506.5

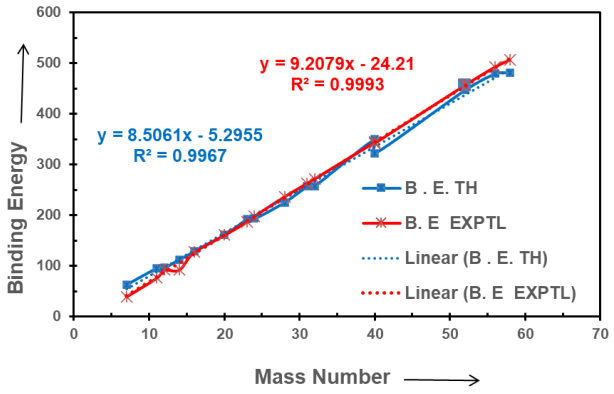

Fig. VII: Plot of Binding Energies for Mass Numbers A ≤ 60

Table IX: Matching of binding energies for nuclides with mass number 60 ≤ A ≤ 200

Isotope	Z	A	B. E. Theo.	B. E. Exp.	Isotope	Z	A	B. E. Theo.	B. E. Exp.
^{64}Zn	30	64	479.4	559.1	^{137}Ba	56	137	1142.1	1149.7
^{75}As	33	75	592.2	652.6	^{140}Ce	58	140	1156.2	1172.7
^{85}Rb	37	85	676.8	739.3	^{152}Sm	62	152	1269.0	1251.1
^{88}Sr	38	88	705.0	768.5	^{158}Gd	64	158	1325.4	1295.9
^{98}Mo	42	98	789.6	864.2	^{166}Er	68	166	1381.8	1351.6
^{106}Pd	46	106	846.0	909.4	^{174}Yb	70	174	1466.4	1406.6
^{112}Cd	48	112	902.4	957.0	^{187}Re	75	187	1579.2	1491.9
^{120}Sn	50	120	987.0	1020.5	^{197}Au	79	197	1663.8	1559.4

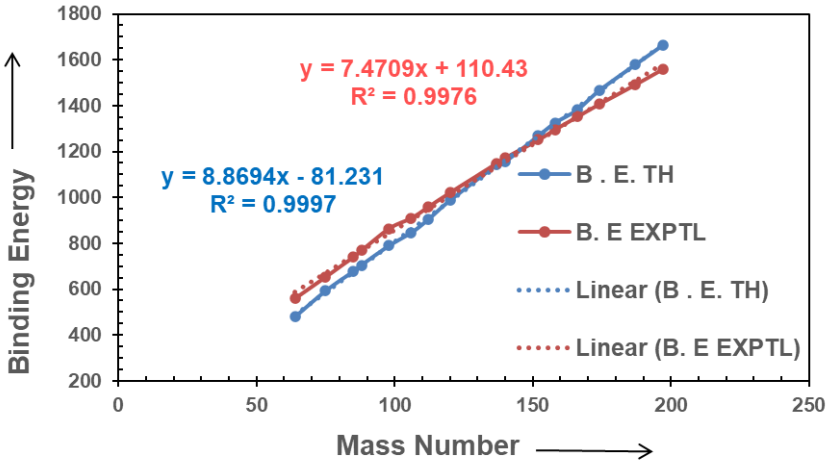

Fig. VIII: Plot of Binding Energies for Mass Numbers $60 \leq A \leq 200$

Table X: Matching of binding energies for nuclides with mass number A >200

Isotope	Z	A	B. E. Theo.	B. E. Exp.	Isotope	Z	A	B . E. Theo.	B. E. Exp.
^{202} Hg	80	202	1518.2	1595.2	^{238} U	92	238	1820.6	1801.7
^{205} Tl	81	205	1543.4	1615.1	^{237}Np	93	237	1793.4	1795.3
^{208} Pb	82	208	1568.6	1636.4	^{243}Am	95	243	1843.8	1829.8
^{209} Po	84	209	1553.5	1637.6	^{247}Cm	96	247	1882.1	1853.0
^{222} Rn	86	222	1695.6	1708.2	^{247}Bk	97	247	1868.0	1852.2
^{223}Fr	87	223	1694.6	1713.5	^{252} Es	99	252	1905.3	1879.2
^{226} Ra	88	226	1719.8	1731.6	^{257} Fm	100	257	1956.7	1907.5
^{232} Th	90	232	1770.2	1766.7	^{258}Md	101	258	1955.7	1911.7

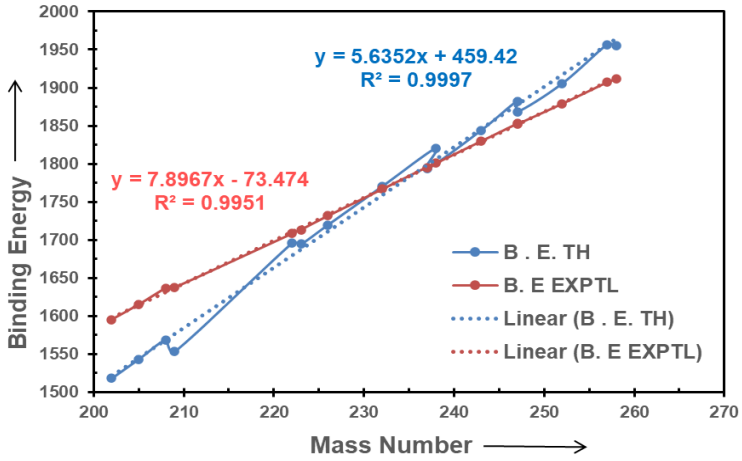

Fig. IX: Plot of Binding Energies for Mass Numbers A >200

To test the proposed empirical equation, some nuclides are chosen at random from the entire range of isotopes of known elements [24] and their calculated and experimental values of binding energy are plotted in Fig. X.

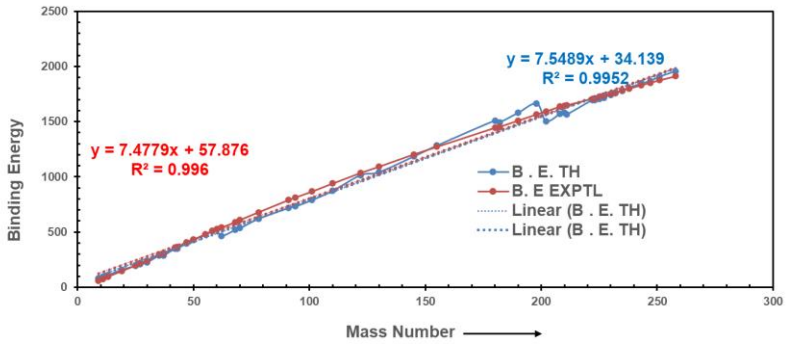

Fig. X: **Plot of Binding Energies for Mass Numbers taken at random**

The closeness as exhibited by the plots reveals that the empirical equations yield satisfactory binding energy values.

Inference:

The nucleus of an atom is a solid entity with uneven density (excepting α particle) in which the nucleons (protons and neutrons) are bonded by a force arising from the exchange of π-meson which is a constituent of the neutron. The binding energy of the nucleons is supplied mainly by the exchange of d-quarks and partly by the Coulombic interaction between d and u-quarks of the bonded nucleons. The role of either gravitational or weak nuclear force seems to be negligible.

It may be considered as a general rule that since nuclides of isotopes differ from one another by the presence of one or more electrons, their binding energies will differ from each other by 14.1 MeV or its multiple with slight deviation due to Coulombic interaction between the quarks. In a similar way, isotonic nuclides which contain the same number of neutrons will

have their binding energies almost same. This is shown to be the case in many examples cited in this communication.

The nucleus is made up of p – n pairs as building blocks with d-quarks as the mortar. It seems that protons and neutrons which are paired with each other do not revolve in separate orbitals in a nucleus save any odd residual nucleon. Spin motion of the nucleons is possible only when it is rotating along its own axis but any orbital revolution around an axis outside the nucleon does not seem probable. A nucleus is neither a gas nor a liquid. It is a solid which does not conform to any known crystal lattice structure. As such, mean free path for the nucleons is not expected but vibrational motion of the p – n bonds is quite possible.

Unlike liquid-drop, gaseous or optical model, this polyhedral model is a non-mathematical one with arrangement of real particles (nucleons) in some symmetrical pattern. But in conformity of the saying in Sanskrit language *"kendragatam Nirbishesham"* which means in English "nothing particular at the centre" or "centrally void", the mathematical centre of the nucleus may be considered as void.

It appears that by invoking rules which guide extra nuclear electrons (orbits, energy and transition) to the nucleons, complication has been invited into the subject. Rules governing nuclear physics may be somewhat different from those of atomic physics (at least in degrees if not in kind).

Conclusion:

The proposed architectural model of the nucleus qualitatively explains almost all the characteristics of the nuclides. These include nucleosyntheses, emission reactions, fission and fusion mechanism, binding force and binding energies, number of stable elements, mechanism of α and β decays etc. The concept of sub-nucleonic particles like quarks has been used for the first time to explain most of these properties. Although the basic idea of a p – n pair termed

PAULION is an imaginary particle which has not been substantiated by any experiment so far, it may be an excited state of deuteron of transitory existence. The model presented here covers some of the aspects of all the presently known models (like liquid drop, shell, optical and collective). In absence of any experimental evidence (eye witness) only characteristic properties (circumstantial evidences) of the nuclei are to be considered which are in favour of the architectural polyhedral model. However, the final verdict is yet to be pronounced.

The architectural model of the nucleus has been adopted to explain the formation and properties of a handful of nuclides on the basis of the symmetrical arrangements of nucleons. The vast majority of the nuculids of the remaining elements and their isotopes can be fitted in this model by considering the symmetrical arrangements of neutrons, α- particles, p – n pairs and n – n pairs either alone or in combination. This aspect of the problem will be addressed in a later communication.

Acknowledgement:

The authors, who are at the fag end of their lives, gratefully acknowledge the service of viXra e-print archive for making this series of papers open to the science minded community at large overcoming the mismatch between the subject (Nuclear Physics) and the discipline of the authors (Chemistry).

References:

1. Gapon, E., Iwanenko D., Zur Bestimmung der isotopenzahl, *Die Naturwissenschaften*, **20**, 792 (1932).
2. Mayer, M. G., On Closed Shells in Nuclei, *Phys. Rev.*, **74**, 235 (1948).
3. Mayer, M.G., Jensen, J.H.D., Elementary Theory of Nuclear Shell Structure, Wiley, New York, NY (1955).
4. Bohr, N., Disintegration of Heavy Nuclei, *Nature*, **143**, 330 (1939).
5. Frenkel, J., On the Splitting of Heavy Nuclei by Slow Neutrons, *Phys. Rev.*, **55**, 987 (1939).
6. Bohr, A., Mottelson, B., Nuclear Structure, Vol. 2, Benjamin, Reading, MA, (1975/1998).

7. Harvey, B. G, Introduction to nuclear physics and chemistry, Englewood Cliffs, N.J., Prentice-Hall (1962).
8. Fernbach, S., Serber, R., Taylor, T. B. The Scattering of High Energy Neutrons by Nuclei, *Phys. Rev.*, **75**, 1352 (1949).
9. Feshbach,H., Porter, C. E., Weisskopf, V. F., Model for Nuclear Reactions with Neutrons, *Phys. Rev.*, **96**, 448 (1954).
10. Brink, D.M., Friedrich, H., Weiguny, A., Wong, C.W., Investigation of the alpha – particle model for light nuclei, *Physics Letters B*, **33**, 143 (1970).
11. Pauling, L. Structural Basis of Neutron and Proton Magic Numbers in Atomic Nuclei, *Nature*, **208**, 174 (1965).
12. Pauling, L., The close-packed spheron model of atomic nuclei and its relation to the shell model, *Proc. Natl. Acad. Sci.*, **54**, 989 (1965).
13. MacGregor, M.H., Evidence for two-dimensional ising structure in atomic nuclei, *Il Nuovo Cimento*, **A36**, 113 (1976).
14. Cook, N.D., Models of the Atomic Nucleus, Unification Through a Lattice of Nucleons, Second Edition, Springer-Verlag Berlin Heidelberg, (2010) p.146.
15. Sen, B.K., Sen, S., Symmetry based Architectural Model to explain Nucleosyntheses, Fission, Fusion and Emission Processes, viXra e-print archive, 2205.0047v1 (2022), http: //viXra.org/abs/2205.0047.
16. Sen, B. K., Mechanism of nucleosynthesis: Formation of lighter nuclei with proton-neutron pair as the building block, viXra e-print archive, 2109.0078v2, (2021), http://viXra.org/abs/2109.0078.
17. Sen, B.K., Sen, S., Probe of the Alpha Particle Conundrum in Terms of Quarks of Quantum Chromo Dynamics, viXra e-print archive, 2208.0042v1(2022), http://viXra.org/abs/2208.0042.
18. Yukawa, H., On the Interaction of Elementary Particles I, *Proc. Phys. Math. Soc. Jap.*, **17**, 48 (1935).
19. Weizsäcker, CF V. "Zur theorie der kernmassen." Zeitschrift für Physik A Hadrons and Nuclei, **96,** 431 (1935).
20. Hofstadter, R., In, "Nuclear radii" in Nuclear Physics and Technology, Vol. 2, Schopper, H., ed., Springer, Berlin, (1967).
21. Fewell, M. P., The atomic nuclide with the highest mean binding energy, *Am. J. Phys*, **63**, 653 (1995).
22. Audi, G. Wapstra, A.H. Thibault, C. The Ame2003 atomic mass evaluation: (II). Tables, graphs and references, *Nucl. Phys A*, **729**, 337 (2003).
23. Shurtleff, R., Derringh, E., The most tightly bound nucleus, *Am J. Phys.*, **57**, 552 (1989).
24. Martin, J. E., Physics for Radiation Protection, 3rd Ed., Appendix B, Atomic Masses and Binding Energies for Selected Isotopes of the Elements pp.616-623, Wiley-VCH, Verlag & Co. KGaA (2013).